

## Supplemental Materials

### Supplemental Methods

#### *Measurement of FGF in Outflow*

We verified that capillary washout of FGF through microvascular clearance was indeed responsible for the reduction in FGF penetration in the presence of perfusion with  $^{35}\text{S}$ -FGF1. Rat hearts were isolated and perfused using identical procedures and experimental parameters described in the “Ex-vivo Myocardial Drug Delivery” methods section for perfused hearts.  $^{35}\text{S}$ -FGF1 (4.2 mg/ml) was applied to the epicardial surface (n=3) for 3 hours. The perfusate in these experiments was not recirculated, hence presence of  $^{35}\text{S}$ -FGF1 in the outflow results from direct washout of exogenous growth factor in tissue. Outflow perfusate was collected in 6-30m fractions. At the end of perfusion experiments, 3ml samples of the outflow fractions were decolorized with 0.5ml hydrogen peroxide at 60°C for 1 hour (30%, Sigma-Aldrich), and assayed for  $^{35}\text{S}$  radioactivity using liquid scintillation counter (Packard).

#### *Continuum Pharmacokinetic Model of Myocardial Drug Transport*

Following Tzafriri et. al.<sup>1</sup> we model interstitial drug transport in a perfused tissue using the classical diffusion equation with a linear sink term

$$\frac{\partial C}{\partial t} - D \frac{\partial^2 C}{\partial x^2} = -kC \quad (\text{S1})$$

where the apparent clearance rate constant  $k$  is proportional to trans-endothelial permeability as

$$k = \frac{P_{mv} S_{mv}}{(1 - \phi_{mv})}. \quad (\text{S2})$$

Here  $S_{mv}$  is the surface fraction of capillaries and  $\phi_{mv}$  is the capillary volume fraction. Since the surface fraction of a cylinder of radius  $R_{mv}$  is related to the volume fraction as  $S_{mv} = 2\phi_{mv} / R_{mv}$  we can rewrite the proportionality between the apparent clearance rate constant and trans-endothelial permeability as

$$k = \left( \frac{2}{R_{mv}} \right) \frac{P_{mv} \phi_{mv}}{1 - \phi_{mv}}. \quad (\text{S3})$$

A rich literature exists on the analysis of Eq. S1. For our purposes, it suffices to note that localization of the experimental growth factor profiles close to the drug source justifies the analysis of distribution profiles in terms of penetration into a semi-infinite domain<sup>2</sup>. Namely, we assume that the concentration of growth factor at the far end of the tissue is negligible

$$C = 0, \quad x = L. \quad (\text{S4})$$

With this in mind, under the conditions of a constant surface concentration

$$C = C_0, \quad x = 0 \quad (\text{S5})$$

the concentration profile takes the form<sup>2</sup>

$$C / C_0 = \frac{1}{2} e^{-x/\ell} \operatorname{erfc} \left( \frac{x}{2\sqrt{Dt}} - \sqrt{kt} \right) + \frac{1}{2} e^{x/\ell} \operatorname{erfc} \left( \frac{x}{2\sqrt{Dt}} + \sqrt{kt} \right). \quad (\text{S6})$$

where

$$\ell = \sqrt{\frac{D}{k}}. \quad (\text{S7})$$

Thus, clearance gives rise to a length scale  $\ell$  that is independent of the dimensions of the tissue and is inversely related to the clearance rate constant. Correspondingly, using Danckwert's method<sup>2</sup> it is possible to show that net tissue deposition  $M$  depends on time as

$$M = C_0 \ell \operatorname{erf}(\sqrt{kt}). \quad (\text{S8})$$

Thus,  $k^{-1}$  operates as the time scale for the tissue to approach its steady state deposition

$$M = C_0 \ell \quad (\text{S9})$$

and distribution

$$C = C_0 e^{-x/\ell}. \quad (\text{S10})$$

Hence, increasing the clearance rate constant results in less drug penetration and more significant localization near the drug source. On the contrary, as the clearance rate constant tends to zero, the limitation on drug penetration is lifted ( $\ell \gg L$ ) such that drug penetration and deposition reduce to the classical linear diffusion limits

$$C/C_0 \approx \operatorname{erfc}\left(\frac{x}{2\sqrt{Dt}}\right) \quad (\text{S11})$$

and

$$M \approx 2C_0 \sqrt{Dt/\pi}. \quad (\text{S12})$$

The preceding analysis wherein the surface concentration was held constant provides insights on drug transport during the initial burst release phase. Subsequently drug release from the polymer device occurs at an essentially constant rate. Consider next the extreme limit wherein the flux  $F_0$  rather than the concentration is held constant at the surface

$$-D \frac{\partial C}{\partial x} = F_0, \quad x = 0 \quad (\text{S13})$$

The steady state distribution of drug implied by Eq. S1 is then

$$C = (\ell F_0 / D) e^{-x/\ell}. \quad (\text{S14})$$

Thus, in the face of first order clearance, steady state drug distribution is always exponential with a length scale  $\ell$ ; device release kinetics is seen to only impact the steady state concentration of drug at the device:tissue interface ( $x=0$ ). Integrating the steady state distribution profile Eq. S14 over the entire tissue we find that steady state tissue deposition  $M$  scales linearly with flux and inversely with the apparent clearance rate constant

$$M = \frac{F_0}{k}. \quad (\text{S15})$$

Using the Danckwert's method<sup>2</sup>, it is possible to derive the time dependent counterpart of Eq S15, as

$$M = \frac{F_0}{K} (1 - e^{-kt}), \quad (\text{S16})$$

thus confirming that  $k^{-1}$  also operates as the time scale for the attainment of steady state tissue deposition when drug is released at a constant flux from the polymeric device.

### ***Analytical Model Calculation of Cumulative FGF Clearance***

Cumulative FGF washout through microvascular clearance, between times  $t_1$  and  $t_2$  can be calculated from the experimental value of clearance constant  $k$  and the total deposition  $M$  (Eqn. S8) by the following relationship:

$$CL = \int_{t_1}^{t_2} k M dt = \int_{t_1}^{t_2} k C_0 \ell \operatorname{erf}(\sqrt{kt}) dt \quad (\text{S17})$$

### ***Recombinant FGF2 Production***

Recombinant FGF2 was expressed in *Escherichia coli* strain FICE-127 transformed by plasmid vector pFC80 that confers resistance to ampicillin and encodes FGF2 under the control of the tryptophan promoter (the transformed FICE-127 strain was a gift from John Heath, University of Birmingham, and was originally constructed by Antonella Isacchi, Amersham Pharmacia Biotech and Upjohn). FICE-127 cells containing pFC80 were inoculated into LB Medium (MP Biomedicals) containing 0.29 mmol/L (10 mg/dL) of ampicillin (Invitrogen) and grown overnight at 37°C in a shaker at 250 RPM. The inoculum was diluted 1:100 in M9 Minimal Medium (Fisher Scientific) containing 1 g/L amino acids (Becton Dickinson) without tryptophan to induce protein production. Cells were grown for 6 h at 37°C in a shaker at 250 RPM. Cells were collected by centrifugation at 8000 RPM for 10 m and kept frozen at -80°C. Frozen cell pellets were resuspended in  $6.94 \times 10^{-2}$  mmol/L (100 mg/dL) lysozyme in GET buffer (100 mmol/L Glucose, 10 mmol/L EDTA, and 50 mmol/L Tris, pH 8.0), vigorously agitated for 5 m and homogenized (Polytron; Kinematica) 5 times for 30 s each with break periods of 60-90 s at 4°C to prevent overheating and denaturation of proteins.

Bacterial lysate was collected by centrifugation at 9,000 RPM for 10 m at 4°C. FGF2 was then purified using affinity chromatography with FPLC (Pharmacia Biotech). Lysate was loaded into 5 mL heparin Sepharose column (HiTrap, GE Healthcare) and allowed to bind for 2 h at 4°C. The FPLC system was programmed to wash the column with phosphate buffered saline (PBS) containing incrementally concentrated NaCl with a linear gradient (150 mmol/L to 2000 mmol/L). Elutions were collected in sequential 1 mL fractions, with FGF2 eluting at 1400 mmol/L to 1600 mmol/L NaCl. The FGF2 solution was desalted by centrifugation using

centrifugal filters with 10 kDa molecular weight cut-off (Centricon, Millipore). After each purification, the presence of FGF2 was confirmed at a 18kDa band using SDS-PAGE, and protein concentration was quantified with a BCA assay (Pierce). Bioactivity of FGF2 was confirmed by in vitro proliferation assays using bovine aortic endothelial cells.

### ***Fluorescence Labeling of FGF2***

A heparin Sepharose column (HiTrap, GE Healthcare) was loaded with 1 mL of 0.12 mmol/L (200 mg/dL) FGF2 in PBS and allowed to bind for 1 h at room temperature. The FGF2-loaded column was washed with 5 mL of 100 mmol/L NaHCO<sub>3</sub> to increase the pH to 8.3 and loaded with 1 mL of 1.60 mmol/L (100 mg/dL) Texas Red succinimidyl ester (Invitrogen). Texas Red succinimidyl ester was allowed to react with FGF2 for 10 m at room temperature. The column was then placed in-line on the FPLC system, and FGF2 was eluted as described above. Elutions of 1 mL were collected and assayed for protein content (absorbance at 280 nm, FPLC System) and Texas Red fluorescence intensity (595 nm/615 nm excitation/emission wavelengths, Fluoroskan II, Lab Systems Oy). Texas Red was appropriately conjugated to FGF2 as indicated by the concurrence of the elution peaks of fluorescence intensity and protein concentration. Both were came off the column between 1400 to 1600 mmol/L NaCl, similar to the elution range of unlabeled FGF2, suggesting that Texas Red conjugation did not change the heparin binding properties of FGF2. Buffer exchange was performed on the Texas Red labeled-FGF2 (TR-FGF2) solution by centrifugation as above. SDS-PAGE indicated that the molecular weight of TR-FGF2 is not significantly different from that of FGF2. Fluorescence intensity was calibrated to protein concentration prior to delivery using microplate fluorometry (Fluoroskan).

### ***Recombinant S35-FGF1 Production***

<sup>35</sup>S-FGF1 was chosen as a model for FGF in the *in-vivo* setting because its high detection sensitivity allows for the possibility of tracking spatial drug distribution in the setting of controlled delivery of therapeutic doses. It also presents a safer alternative to using <sup>125</sup>I labeled FGF2 *in-vivo*. Recombinant human FGF1 was expressed in *Escherichia coli* strain BL21-pLysS transformed by plasmid, pET3c that confers resistance to ampicillin and encodes FGF1 (obtained as a gift from the late Dr. Thomas Maciag, Maine Medical Center, Portland, ME). Transfected bacteria stocks were added to LB medium (MP Biomedicals) containing 100 µg/mL Carbenicillin and 35 µg/mL Chloramphenicol (Sigma-Aldrich) and incubated with vigorous shaking at 250 RPM at 37°C overnight. Bacteria culture was then diluted in antibiotics-free LB medium (1:40 v/v of bacteria/medium) and incubated with vigorous shaking at 250 RPM and the optical density of the solution was measured at 600 nm. When cell culture reached an optical density of 0.6-0.8 bacteria were centrifuged and resuspended in DMEM medium deficient in L-cysteine and L-methionine (Invitrogen) supplemented with 1 % L- glutamine and 7.15 mCi of <sup>35</sup>S (Promix L-[<sup>35</sup>S]Methionine and Cysteine, GE Healthcare Life Sciences) and buffered with 25 mM HEPES (Invitrogen) and then induced with 0.4 mM IPTG for 3 h with shaking at 250 RPM at 37°C. Cells were then collected by centrifugation at 8000 RPM for 10 m and kept frozen at -80°C.

Frozen cell pellets were resuspended in 1mg/ml lysozyme in GET buffer (50 mM Tris, 10 mM EDTA, 100 mM glucose, pH 8.0), mixed well for 5 m and then homogenized (Polytron; Kinematica) 5 times for 30 s each with break periods of 60-90 s at 4°C to prevent overheating and denaturation of proteins. Cell lysate was collected by centrifugation at 9,000 RPM for 10 m

at 4°C. <sup>35</sup>S-FGF1 was then purified using affinity chromatography with FPLC. Bacterial lysates were loaded into 5 ml heparin sepharose column (HiTrap Heparin HP column, GE Healthcare Life Sciences) and allowed to bind for 1 h at room temperature. The FPLC system was programmed to wash the column with PBS and gradually increase NaCl concentration with a linear gradient (0.15-2 M). Elutions of 1 mL were collected and assayed for protein concentration (absorbance at 280 nm, FPLC System) and radioactivity (2500TR Liquid Scintillation Analyzer, Packard). Elution peaks of protein concentration and radioactivity coincided. The <sup>35</sup>S protein product came out of the heparin sepharose column at 1.4 M to 1.6 M NaCl, similar to FGF1, and indicating <sup>35</sup>S was incorporated in FGF1. <sup>35</sup>S-FGF1 solution was desalted by centrifugation using centrifugal filter devices with a 10 kDa molecular weight cut-off (Centricon, Millipore). After each purification, the presence of FGF1 was confirmed at a 18 kDa band using SDS-PAGE and protein quantification was carried out using BCA assay (Pierce). Bioactivity of FGF1 was confirmed in proliferation assays of bovine aortic endothelial cells. FGF1 was further purified from any endotoxin contamination using endotoxin removing columns (Detoxi-Gel AffinitiPak columns, Pierce), and the FGF1 purity was confirmed with limulus ameocyte lysate assay (Pyrotell-T, Associates of Cape Cod Inc., MA). Purification was continued (typically 2-3 times) until endotoxin concentration is below 0.01 EU/μg FGF1.

### ***Fabrication and Kinetics of Controlled Release Device***

A slurry mixture of heparin-Sepharose beads/alginate solution was prepared by mixing sterilized heparin-Sepharose microbeads (GE Healthcare) with filter-sterilized sodium alginate (Sigma-Aldrich, 5 %), placed in a customized 20mm × 20mm × 1mm glass mold, and incubated overnight in filter-sterilized 10 % CaCl<sub>2</sub>. The heparin-Sepharose embedded sodium alginate



material is exposed to  $\text{CaCl}_2$  through two open surfaces of the mold. The gel was further incubated in the 10 %  $\text{CaCl}_2$  for 24 h to allow thorough cross-linking of the polymer after being taken out of the mold under UV light for sterilization. The hardened polymeric gel device was then incubated in  $^{35}\text{S}$ -FGF1 solution for 48 h prior to experiment to allow complete and uniform loading of drug.

To characterize  $^{35}\text{S}$ -FGF1 release kinetics from the device, 8 mm diameter circular shape devices were made from the  $20 \times 20 \times 1 \text{ mm}^3$  polymeric slab using 8 mm biopsy punch (Miltex). These circular devices were incubated in 1 ml PBS and gently agitated throughout the experiment with a shaker. At various time points the elution mixture was collected and assayed for  $^{35}\text{S}$  activity using liquid scintillation counter (Packard). Fresh PBS was used to renew the elution buffer.

## Supplemental Results

### *FGF is Washed-out Through Microvascular Clearance Followed Ex-vivo Myocardial Delivery*

<sup>35</sup>S-FGF1 was observed in the perfusate at the outflow soon after <sup>35</sup>S-FGF1 was delivered at epicardial surface (Figure S2), suggesting that capillary washout was indeed responsible for the limited penetration of this growth factor in the presence of perfusion (Figure 1). These results were further compared to analytical model results of cumulative drug clearance (Eqn S17) calculated using pharmacokinetic parameters of FGF-2 ( $k = 1.15 \pm 0.06 \times 10^{-4} \text{ s}^{-1}$  and  $D = 0.02 \text{ } \mu\text{m}^2/\text{s}$ ) derived from experiment. The experimental results fit the model well within one order of magnitude, suggesting that the pharmacokinetics of <sup>35</sup>S-FGF1 are well explained by our diffusion with clearance model and moreover that the clearance constants and diffusivities of <sup>35</sup>S-FGF1 and TR-FGF2 are similar.

## Figure Legends:

**FIGURE S1: Isolated perfused heart apparatus.** Rat coronary arteries were perfused antegrade through an aortic canula at constant physiologic mean pressure while a constant, well mixed drug source was applied to the epicardial surface. Spatial drug distribution was quantified in myocardial tissue regions exposed to drug. High magnification schematic illustrates the examined physiologic forces: drug diffusion within tissue and clearance through convection by intravascular flow after permeation across capillary wall.

**FIGURE S2: FGF is Washed-out Through Microvascular Clearance Followed Ex-vivo Myocardial Delivery.**  $^{35}\text{S}$ -FGF1 in the outflow perfusate was measured as a function of time after local epicardial  $^{35}\text{S}$ -FGF1 delivery (n=3). Experimental washout of  $^{35}\text{S}$ -FGF-1 (in blue) is well explained by Eq. S17 (magenta line) using the parameter values of TR-FGF2.

## References

1. Tzafriri AR, Lerner EI, Flashner-Barak M, et al. Mathematical modeling and optimization of drug delivery from intratumorally injected microspheres. *Clin Cancer Res.* Jan 15 2005;11(2 Pt 1):826-834.
2. Crank J. *The mathematics of diffusion*. 2d ed. Oxford, [Eng]: Clarendon Press; 1979.

FIG-S1

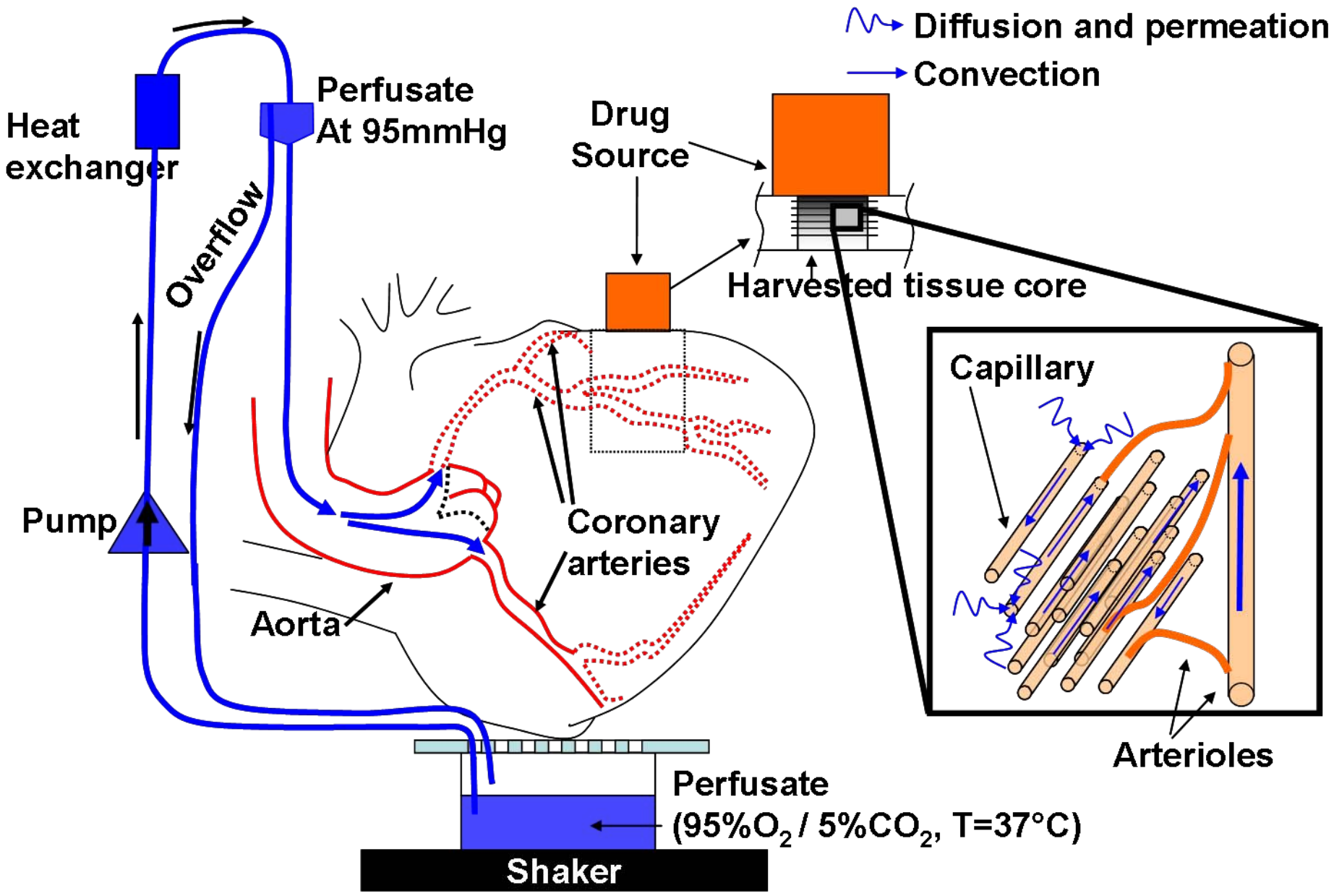


**FIG-S2**

